8th International Conference on Multiphase Flow
ICMF 2013, Jeju, Korea, May 26 - 31, 2013

Simulation of coalescence, break up and mass transfer in bubble columns by using the Conditional Quadrature Method of Moments in OpenFOAM

Antonio Buffo[1], Daniele L. Marchisio[1],Marco Vanni[1], Peter Renze[2]

[1]*Department of Applied Science and Technology, Politecnico di Torino, Torino, Italy*
[2]*Multiphase Flows Group, BASF SE, Ludwigshafen, Germany*

Keywords: bubbly flows, CFD, multiphase flows, conditional quadrature method of moments

Abstract

The evaluation of the mass transfer rates and the fluid-dynamics aspects of bubble columns are strongly affected by the intrinsic poly-dispersity of the gas phase, namely the different dispersed bubbles are usually distributed over a certain range of size and chemical composition values. In our previous work, gas-liquid systems were investigated by coupling Computational Fluid Dynamics with mono-variate population balance models (PBM) solved by using the quadrature method of moments (QMOM). Since mass transfer rates depend not only on bubble size, but also on bubble composition, the problem was subsequently extended to the solution of multi-variate PBM (Buffo *et al.* 2013). In this work, the conditional quadrature method of moments (CQMOM) is implemented in the open-source code OpenFOAM for describing bubble coalescence, breakage and mass transfer of a realistic partially aerated rectangular bubble column, experimentally investigated by Diaz *et al.*(2008). Eventually, the obtained results are here compared with the experimental data available.

Introduction

The simulation of gas-liquid flows is very important in the process industry since many important chemical reactions (e.g., oxidations, hydrogenation) are usually carried out by means of different gas-liquid contactors, such as bubble columns and aerated stirred tanks.
These systems have been widely investigated with CFD by using different multiphase models; notably the multi-fluid approach represents the only feasible way to predict the fluid dynamic behavior of entire industrial scale equipments in terms of computational costs. Nevertheless all these models are based on the a priori assumption of a local mean bubble size and limited by the fact that such value is kept constant throughout the computational domain and during all the simulation time.
It is intuitive to think that bubbles in liquids are not monodispersed, but their properties, such as size, shape, velocity, chemical composition, etc..., may be distributed over different values. Such distributions of these so-called internal coordinates can be theoretically described by means of a PBM approach: the local bubble population is described through a NDF that may change in space and time according to the PBE, where the relevant phenomena are accounted for. For gas-liquid systems the most important phenomena are the bubble motion in physical space considering the different interfacial forces acting on bubbles, bubble growth or shrink due to molecular processes (e.g., evaporation, condensation, mass transfer or chemical reactions), bubble coalescence and breakage consequent to bubble collisions.
The main limitation of standard multi-fluid models can be thus overcome by coupling the PBM approach with the CFD description: QBMM introduced by Marchisio *et al.* (2003) and Marchisio and Fox (2005) represent a good trade-off between accuracy and computational costs. These methods, implemented in the commercial CFD code ANSYS Fluent, were recently employed to describe the behavior of an aerated stirred tank reactor, focusing on the fluid dynamics aspects given by considering the size polydispersity with QMOM (Petitti *et al.* 2009) and on the validation of model predictions through comparison with the experimental data available of local bubble size distributions (Petitti *et al.* 2010). More recently, the solution methods were extended in order to consider both size and composition distribution to describe in detail the mass transfer process: DQMOM and CQMOM were both implemented and compared (Buffo *et al.* 2011, 2012), showing that CQMOM is more suitable for gas-liquid systems (Buffo *et al.* 2013).
In this work, the CQMOM implementation in the open-source code OpenFOAM is used to simulate bubble coalescence, breakage and mass transfer in a real pseudo 2-D bubble column (Diaz *et al.* 2008) for which experiments are available for model validation.

Nomenclature

a	Specific surface area of bubbles (1/m)
C_{O_2}	Oxygen concentration (mol/m^3)
G	Rate of bubble growth (m/s)
h	Collisional term of PBE (1/m^{3}s)
L	Bubble size (m)
k_L	Mass transfer coefficient (m/s)
k_V	Volumetric shape factor (-)

m	Mean of the distribution (-)
$M_{k,l}$	Generic moment of the NDF($m^k mol^l/m^3$)
n	Number density function ($1/m^4 mol$)
N	Number of nodes of quadrature (-)
t	Time (s)
$\mathbf{u}$	Bubble velocity (m/s)
U	Generic velocity (m/s)
v	Variance of the distribution (-)
$\boldsymbol{x}$	Spatial coordinates

Greek letters

α	Gas volume fraction (-)
μ	First parameter of the log-normal distribution (-)
σ	Second parameter of the log-normal distribution (-)
ϕ	Bubble composition (mol)
$\dot{\phi}$	Rate of mass transfer (mol/s)

Subsripts

G	Gas phase
k	Order with respect to bubble size
l	Order with respect to bubble composition
in	Inlet
r	Relative

Acronyms

CFD	Computational fluid dynamics
CQMOM	Conditional quadrature method of moments
DQMOM	Direct quadrature method of moments
NDF	Number density function
PBE	Population balance equation
PBM	Population balance model
PDF	Probability density function
POP	Plume oscillation period
QBMM	Quadrature-based moment methods
QMOM	Quadrature method of moments

Model Description

The Eulerian-Eulerian approach is here used to simulate the gas-liquid system, considering both phases as incompressible. Although many different interfacial forces determine the fluid dynamic behavior in bubble columns, here only drag, gravity and buoyancy forces are considered in first approximation. The drag coefficient is evaluated assuming a unique value of terminal velocity for all the bubbles equal to 20 cm/s, accounting for the damping effect of turbulence and swarm of bubbles on the bubble slip velocity (for details see Petitti *et al.* 2009, 2010). The *k-ε* model for turbulent multiphase systems formulated by Kataoka and Serizawa (1989) is adopted since represents a good trade-off between accuracy and computational costs.
The bubble population is described through a number density function, so that the following quantity

$$n(L, \phi; \mathbf{x}, t)\mathrm{d}\phi\ \mathrm{d}L$$

represents the expected number of bubbles per unit volume d$\mathbf{x}$ at time t with size ranging between L and L+dL and composition ranging between ϕ and ϕ+dϕ. In this work, an isothermal air-water system is investigated and composition is described by using the absolute number of moles of the chemical component contained in the bubble (i.e., in this case only oxygen). It is possible to write the continuity statement of NDF, the so-called PBE, in the following way:

$$\frac{\partial n}{\partial t} + \nabla \cdot (\mathbf{u}\, n) + \frac{\partial}{\partial L}(G\, n) + \frac{\partial}{\partial \phi}\left(\dot{\phi}\, n\right) = h \qquad (1)$$

where $\mathbf{u}$ is the velocity of the bubbles (calculated here with solving additional equations corresponding to the well-known multi-fluid model), G represents the continuous rate of change of bubble size due to mass transfer, $\dot{\phi}$ is the continuous rate of change of bubble composition due to mass transfer and h is the functional related to the discontinuous jump in bubble size and composition due to collisional events, as coalescence and break up. Sub-models are needed to express these terms; details regarding the formulation can be found elsewhere (Buffo *et al.* 2013). It is important to mention that all these sub-models are based on the local value of the turbulent dissipation rate, provided here by the solution of the multiphase *k*-ε model. The mass transfer rate (and so the continuous change of bubble size) was estimated by means of the Danckwerts' penetration theory, in particular by considering the eddy renewal time equal to the Kolmogorov time-scale as prescribed by the Lamont and Scott model (Lamont and Scott, 1970). Here the turbulent fluctuation is considered as the only mechanism responsible of bubble coalescence and breakage; the coalescence efficiency is evaluated as the ratio between the contact and drainage time-scales, whereas bubble break up is assumed to resultalways in two bubbles with different sizes (prescribed by a β-PDF daughter distribution function) and equal oxygen concentration.
Recurring to the definition of the mixed order moment of the NDF:

$$M_{k,l}(\mathbf{x}, t) = \iint_0^{+\infty} n(L, \phi; \mathbf{x}, t) L^k \phi^l \,\mathrm{d}L\ \mathrm{d}\phi, \qquad (2)$$

it is possible to rewrite Eq. (1) in terms of mixed order moment as follows:

$$\frac{\partial M_{k,l}}{\partial t} + \nabla \cdot \left(\mathbf{u}_{k,l} M_{k,l}\right) + \int_0^{+\infty} k\, L^k (G\, n)\,\mathrm{d}L + \int_0^{+\infty} l\, \phi^l \left(\dot{\phi}\, n\right)\mathrm{d}\phi = h_{k,l},$$

where the velocity of the generic moment $\mathbf{u}_{k,l}$ and the collisional term $h_{k,l}$ are defined below:

$$\mathbf{u}_{k,l} = \frac{\iint_0^{+\infty} \mathbf{u}\, n\, L^k \phi^l \mathrm{d}L\ \mathrm{d}\phi}{M_{k,l}},$$

$$h_{k,l} = \iint_0^{+\infty} h\, L^k \phi^l \,\mathrm{d}L\ \mathrm{d}\phi.$$

As observed initially by Hulburt and Katz (1964), there is a closure problem in the derived transport equation for the moments: in fact the functional form of the NDF is in general unknown. As suggested by Yuan and Fox (2011), this problem is overcome by assuming the following functional assumption for the NDF:

$$n(L,\phi) = \sum_{i_1=1}^{N_1} \sum_{i_2=1}^{N_2} w_{i_1}\, w_{i_1,i_2}\, \delta[L - L_{i_1}]\delta[\phi - \phi_{i_1,i_2}] \quad (4)$$

where the N_1 weights w_{i_1}, the N=N_1N_2 conditional weights w_{i_1,i_2} and the N nodes of quadrature $[L_{i_1};\ \phi_{i_1,i_2}]$ are calculated from a specific set of mixed order moments with an efficient algorithm formulated by Yuan and Fox (2011). As it is possible to notice in Eq. (4), N_1 is the number of nodes used for size and N_2 for the composition conditioned over the i_1-th value of size. An illuminating example is represented by the case with N_1=3 and N_2=1: four pure moments with respect to size are needed to calculate the three weights w_1, w_2 and w_3 and the three nodes L_1, L_2 and L_3 (i.e., $M_{0,0}$, $M_{1,0}$, $M_{2,0}$, $M_{3,0}$, $M_{4,0}$, $M_{5,0}$), then another three mixed-order moments are needed to calculate the three conditional weights $w_{1,1}$, $w_{2,1}$ and $w_{3,1}$ and conditional nodes $\phi_{1,1}$, $\phi_{2,1}$ and $\phi_{3,1}$ (i.e., $M_{0,1}$, $M_{1,1}$, $M_{2,1}$). A detailed description of the algorithm can be found in the work of Buffo *et al.* (2013).

Test case and numerical details

The simulated experimental apparatus consists of a 0.2 m wide, 1.8 m high and 0.04 m deep polymethyl methacrylate partially aerated bubble column, experimentally investigated in the work of Diaz *et al.* (2008). The column was filled with tap water up to 0.45 m from the bottom at room temperature and atmospheric pressure, while the air was fed through an aluminum sparger composed of eight centered holes of 1 mm of diameter and 6 mm pitch. The superficial gas velocity U_G was varied from 2.4 to 21.3 m/s.
Comparison with the numerical simulations is carried out between different sets of experimental data:
• Global gas hold-up, measured through the manometric method, that evaluates the static pressure difference between two pressure sensors located at the wall of the column.

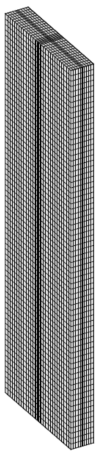

Figure 1: Non uniform hexaedrical mesh used in all simulations (32x11x70).

• Plume Oscillation Period (POP), performed by means of the transformation of the pressure time series from the time domain to the frequency domain and the subsequent identification of the characteristic frequency of the peak in the low frequency band (0 -1 Hz).
• Visual observations, carried out by means of a digital video system.
•Mean Sauter diameter (d_{32}), obtained after manipulation of high-speed digital camera frames through an image processing software. Although the exact coordinates of camera position are not reported, this value probably refers to the situation in the central part of the column in terms of Bubble Size Distribution (BSD).
• Dissolved Oxygen (DO) curves, measured through an oxygen probe inserted in the column in the liquid phase.

Table 1: Numerical schemes and boundary conditions adopted in the simulations.

Variable	Scheme	Inlet	Outlet	Walls
α_G	Limited second order upwind	0.5	Zero gradient	Zero gradient
Gas velocity	Limited second order upwind	Depends on flow rate	Zero gradient with backflow	Free-slip walls
Liquid velocity	Limited second order upwind	0.0 m/s	Zero gradient	No-slip walls
Pressure	First order upwind	Zero gradient	1 bar	Zero gradient
k	Limited second order upwind	Based on turbulent intensity equal to 5% and length scale equal to the hole diameter	1×10^{-4} m^2/s^2 (only backflow)	Zero gradient
ε	Limited second order upwind		1×10^{-5} m^2/s^3 (only backflow)	Zero gradient
Moments	First order upwind	Log-normal distribution	Zero gradient	Zero gradient

TheOpenFOAM solver compressibleTwoPhaseEulerFoam, present in the standard distribution and based on the two-phase Eulerian-Eulerian equations for compressible systems, was modified in order to include a Population Balance module. An implementation of the Conditional Quadrature Method of Moments (CQMOM) was performed and verified, then the obtained results were eventually compared with the experimental data available.
A scheme of the computational mesh is reported in Fig. 1, while spatial discretization schemes and boundary conditions are summarized in Table 1. In all cases the investigated system was composed of tap water and air; standard physical properties of these phases were considered. An adaptive version of the first order backward Euler discretization scheme was used for time integration: the time step Δt is chosen so that the following Courant-Friedrichs-Lewy condition is respected:

$$\mathrm{CFL} = \Delta \mathrm{t} \sum_{i=1}^{3} \frac{U_{r,i}}{\Delta x_i} < 1,$$

where $U_{r,i}$ is the relative velocity between gas and liquid in the i-th direction and Δx_i is the cell size in the same

direction. However, for the sake of numerical stability, the value of Δt cannot be larger than 0.025 s.
It is worth discussing the inlet condition for the gas phase: the gas sparger was modeled through a rectangle with an area equal to the total area enclosed by the 8 holes. The volume fraction of gas α_G imposed on this surface is fixed and equal to 0.5 in all the performed simulations; the inlet gas velocity U_{in} was calculated according to the following expression:

$$U_{in} = \frac{Gas\ flow\ rate}{Sparger\ area\ \times Gas\ vol.frac.}$$

The complex mechanism of bubble formation and detachment from the hole of the sparger was modeled by assuming a log-normal distribution as inlet BSD, according to the work of Petitti *et al.* (2010). The generic mixed order moment was calculated as follows:

$$M_{k,l} = M_{0,0}(k_V C_{O_2})^l \exp\left\{(k+3l)\mu + \frac{(k+3l)^2\sigma^2}{2}\right\}$$

where $M_{0,0}$ is the moment of order zero, namely the total number of bubbles per unit volume, k_V is the volumetric shape factor (equal to π/6 for a sphere), C_{O_2} is the inlet oxygen concentration (equal to 8.56 mol/m^3 for air at 25 °C and atmospheric pressure) and μ and σ are the two parameters of the log-normal distribution. By assuming the mean m of the bubble distribution equal to the bubble diameter calculated with the correlation of Geary and Rice (1991) valid for holed spargers and the standard deviation $\sqrt{v}$ of the distribution equal to 15% of the mean value m as in the works of Laakkonen *et al.* (2007), it is possible to calculate μ and σ in the following way:

$$\mu = \log\left(\frac{m^2}{\sqrt{v+m^2}}\right)$$

$$\sigma = \sqrt{\log\left(\frac{v}{m^2}+1\right)}$$

The value of the moment of order zero $M_{0,0}$ can be calculated by considering the following equality:

$$Gas\ vol.frac. = k_V M_{3,0} = k_V M_{0,0} \exp\left\{3\mu + \frac{9\,\sigma^2}{2}\right\}$$

where $M_{3,0}$ is the moment of order three with respect to bubble size and zero with respect to composition.
Five different superficial velocities U_G were simulated (i.e., 2.4, 7.9, 11.9 16.6, 21.3 mm/s), in order to compare the obtained results with the experimental data available.

Results and Discussion

Important qualitative indications about the prediction given by the model are obtained when some experimental camera frames of the characteristic flow inside the column are compared with the simulation results of gas hold-up and water superficial velocity for different values of the superficial gas velocity U_G.

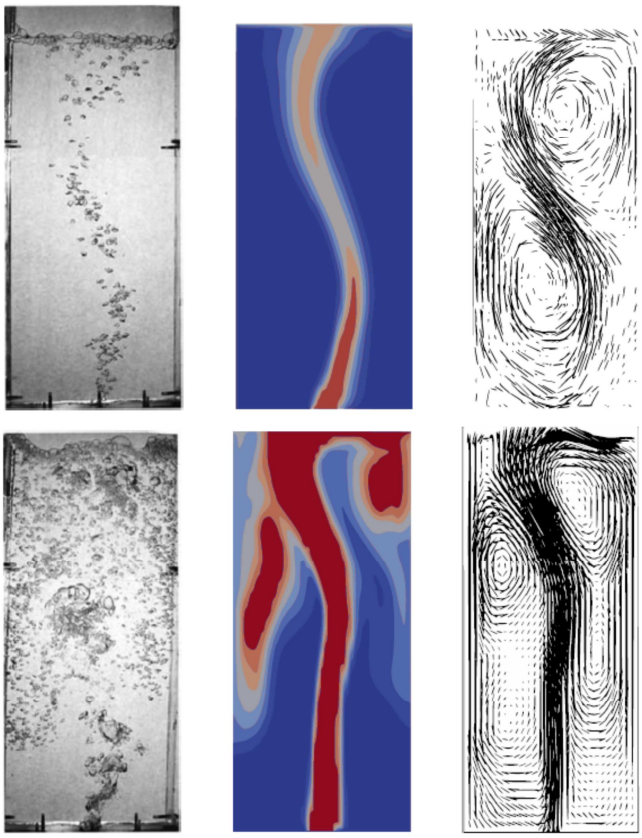

Figure 1: Comparison between experimental and simulation frames at two different superficial velocities. First row: U_G equal to 2.4 mm/s. Second row: U_G equal to 21.3 mm/s. From left to right: high speed camera frame. Gas hold-up distribution [0 (blue), > 0.1 (red)]. Water superficial velocity field.

As it is possible to see in Fig. 1, the simulations are able to predict the central bubble plume and its oscillating motion from side to side of the column. The liquid phase descends along the sidewalls without escaping from the domain due to the fact that the walls are higher than the free surface, allowing the conservation of the total mass of liquid, an aspect of crucial importance in the prediction of mass transfer rates (Buffo *et al.*, 2012). Moreover, it is also clear that the local value of gas hold-up at different U_G is in good agreement with the experimental pictures: for all the simulated cases the region with the highest bubble density is located in the central part of the column where the bubble plume is present. At the lowest gas flow rate bubbles are not trapped into the liquid recirculation motions near walls and tend to stay only in the central region and spread over all the column section only when the plume approaches the free surface. As the superficial velocity U_G is increased to higher values, as clearly seen in Fig.1, smaller bubbles tend to move with the liquid vortices downwards along the side walls, resulting in a better aeration in the bubble column.

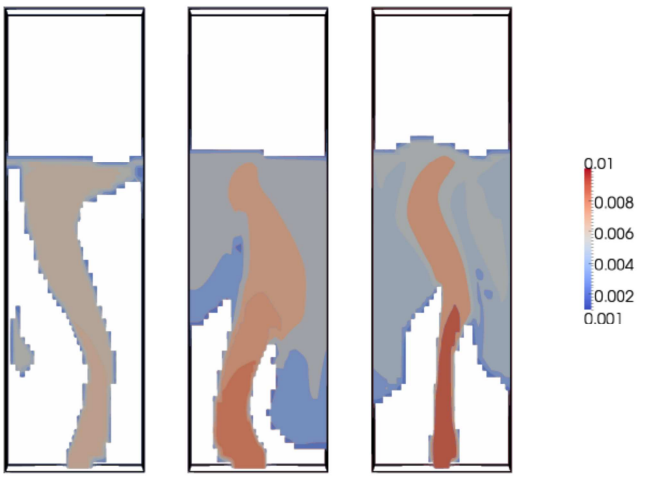

Figure 2: Contour plot of mean Sauter diameter d_{32} for different superficial velocity U_G. From left to right: 2.4 mm/s, 11.9 mm/s, 21.3 mm/s. Units in meter.

This situation is also confirmed by the plot of the liquid velocity field and the profile of the Sauter mean bubble diameter, d_{32} (Fig. 2), calculated as a ratio between the pure moment of order three with respect to bubble size and the pure moment of order two with respect to bubble size. Contour plots of d_{32} show that, with the increase of the gas superficial velocity, smaller bubbles tend to stay in the liquid recirculation path, whereas bigger bubbles are concentrated into the central plume zone where coalescence and breakage occur with faster rates due to the higher turbulent fluctuations.

Table 2: Comparison of experimental data and calculated results for global gas volume fraction (hold-up), POP and mean Sauter diameter varying the superficial gas velocity U_G.

U_G	Hold-up	POP (s)	d_{32} (mm)
2.4	0.62 %	10.10	6.01
Exp.	0.69 %	11.37	6.83
7.1	1.61 %	8.26	6.28
Exp.	1.81 %	5.69	7.05
11.9	2.45 %	5.83	6.89
Exp.	2.63 %	4.27	6.50
16.6	3.36 %	3.80	7.01
Exp.	3.36 %	3.01	6.40
21.3	4.19 %	1.84	7.96
Exp.	4.10 %	2.84	7.73

Another comparison between simulations and experiments is shown in Table 2, where a number of global variables of the column (gas hold-up, POP and mean Sauter diameter) are reported as a function of the superficial gas velocity U_G. In Fig. 3 the measured global gas hold-up values are compared with the predicted ones. As it can be clearly seen, very good agreement is detected both in terms of absolute values and trends; similar trends can be explained by the existence of a unique flow regime, the so-called vortical flow regime (Diaz *et al.*, 2008), as clearly visible in Fig. 1. Furthermore, a similar agreement proves that the choice of the drag model is appropriate, at least for the operating conditions investigated: it is important to remark here that the bubble size diameter is no longer used as a model fitting parameter for catching the experimental value of global gas hold-up, but it is calculated through PBM. As already mentioned, the terminal velocity of the bubble U_T is here assumed equal to 20 cm/s for all the bubbles: the experimentally measured rising velocity of a single bubble in stagnant water is about 25 cm/s for bubble sizes ranging between 2-10 mm (Clift *et al.*, 1978), but this value must be in some way reduced in order to account for the effect of other bubbles (i.e., the local gas volume fraction) and of turbulence of the system (Montante *et al.*, 2007; Petitti *et al.*, 2010). In this case it is possible to state that 20 cm/s is an appropriate value for the system under investigation.

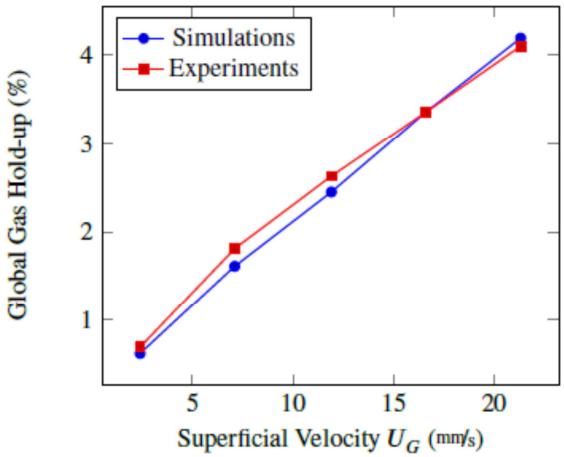

Figure 3: Comparison between experimental data and predicted global gas hold-up for different gas superficial velocities.

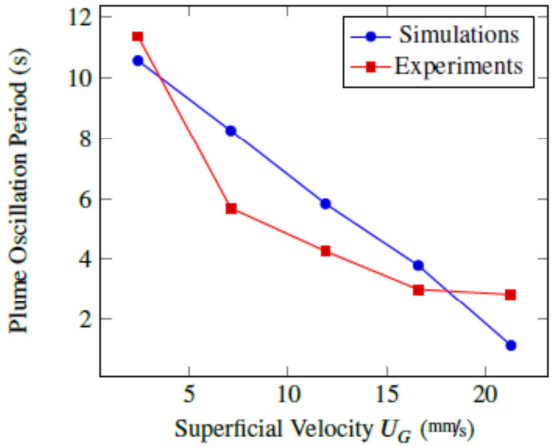

Figure 4: Comparison between experimental data and predicted Plume Oscillation Period for different gas superficial velocities.

In Fig. 4 the comparison between experimental and predicted POP values is reported. As it is possible to see from the experimental observations, at low U_G values, the POP is high and rapidly decreases as gas superficial velocity decreases, until a constant value is reached. This evolution has been related to the evolution of the bubble size

distribution, as coalescence and breakage rates rapidly increase at low gas superficial velocity but then reach a pseudo steady-state at higher U_G values (Buwa and Ranade, 2002). As shown in Fig. 4, the model predictions do not fully capture this trend and the calculated POP decreases almost monotonically with the gas superficial velocity, although the numerical values are comparable. Beyond the difficulty to extract a value from the simulations at higher superficial velocity, when the motion of the bubble plume starts to be chaotic, these results can be explained by the turbulence model used in the predictions, which seems to be not adequate to describe systems characterized by a weak turbulent behavior.

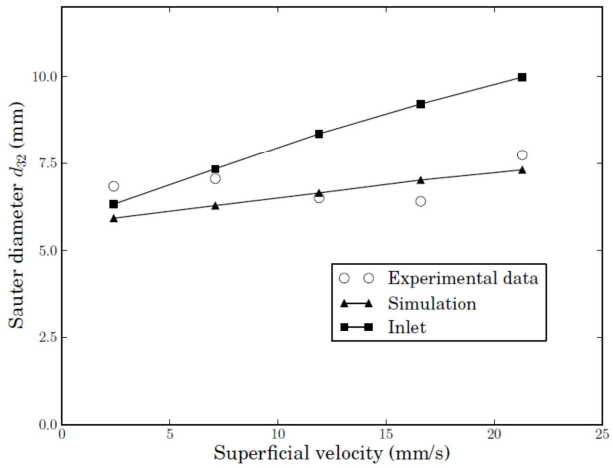

Figure 5: Comparison between experimental and predicted mean Sauter diameter at the center of the column and the inlet value calculated with the correlation of Geary and Rice (1991) d_{32} (mm) for different superficial gas velocities.

Fig. 5 shows the evolution of the mean Sauter diameter d_{32} with respect to the gas superficial velocity. As it was previously pointed out, the exact position of the camera used in the experiments is unknown. For this reason the comparison with the experiments should not be intended here as a validation but only as a qualitative feedback for CQMOM results. More interesting is the comparison between the predicted d_{32} and the value imposed at the inlet and calculated by the Geary and Rice correlation: the average bubble size at the center of the column increases much less with the gas flow rate than the bubble size at the inlet. This fact evidences that the relative importance of break-up process over coalescence increases with U_G, due to the enhancement of turbulent induced collisions at higher gas flow rates.

In Fig. 6 a preliminary result in terms of the mass transfer rate for gas superficial velocity equal to 2.4 mm/s is reported. As soon as the air enters the column, the concentration of oxygen in the liquid phase begins to increase as a consequence of the mass exchange between phases. However the equilibrium is still far to be reached since the investigated system requires the achievement of long simulation times, and therefore the aspects relating to the code optimization are of crucial importance. Another significant result of the mass transfer test is shown in Fig. 7, where the contour plot the local value of global mass transfer coefficient k_La is reported for two different operating conditions. This value differs strongly from point to point into the reactor, because of the turbulence induced by the chaotic motion of the bubbles. In fact, the bubbles present in the plume zone are forced to break-up by turbulence shear stresses, increasing their number and reducing their size. This effect is more evident increasing the gas flow rate, as pointed out in Fig. 5. On the contrary, the portion of volume in the bottom of the column, around the inlet zone is not interested by the gas recirculation and the global mass transfer coefficient tends to zero. It is worth reminding that most of these effects related to bubble coalescence and breakage would not be properly described without a PBM approach.

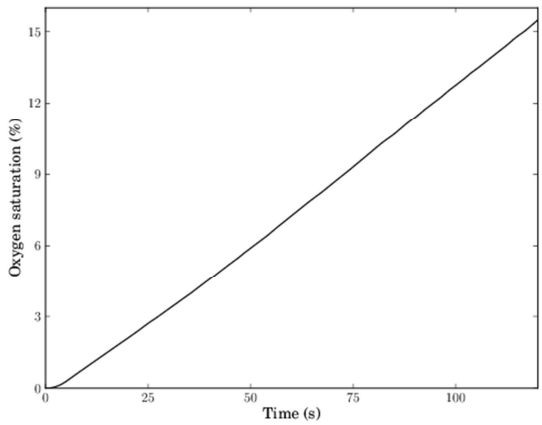

Figure 6: Time evolution of the dimensionless oxygen concentration in the liquid. U_G = 2.4 mm/s

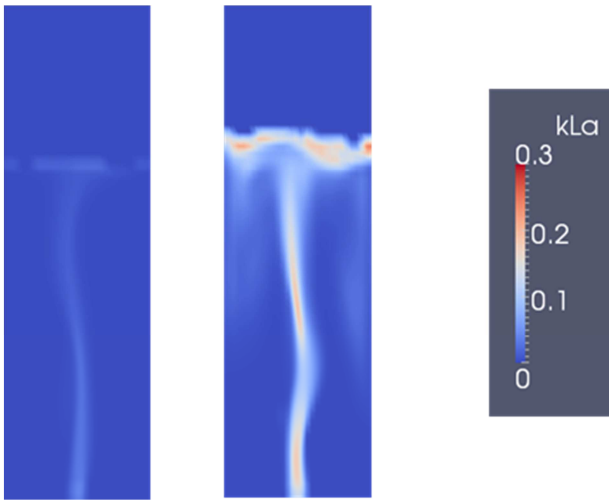

Figure 7: Contour plots of global mass transfer coefficient, k_La (1/s), for two different operating conditions. Left: U_G=2.4 mm/s. Right: U_G=21.3 mm/s.

Conclusions

In this work, CQMOM was implemented in the open source CFD code OpenFOAM, overcoming all the issues that may

arise when new equations must be solved and coupled with the fluid dynamic description in a commercial CFD code. The code obtained from the modification of the standard solver compressibleTwoPhaseEulerFoam is stable and parallelized, providing a solid base for further developments.

For assessing the reliability of the implementation, the partially aerated rectangular bubble column investigated experimentally by Diaz *et al.* (2008) was modeled and the obtained results were compared with the experimental data available at different superficial gas velocities. The performed analysis shows that there is in general a good agreement with the experiments for the compared variables: the trend of global gas hold-up with respect of U_G was correctly reproduced by the model, while the comparison of POP and mean Sauter diameter is still satisfactory despite of the approximations introduced by the model and the impossibility of extracting data from simulations with the same procedures used in the experiments.

Moreover, it was shown that the calculated moments of the bubble size distribution may give detailed and local information of the surface area between the two phases, necessary for carrying out mass transfer simulations of oxygen in water. The smaller bubbles have higher mass transfer rates than larger ones because of a higher interfacial area and tend to reach the equilibrium with the liquid more quickly; for this reason not only the bubble size, but also bubble concentration is needed for a proper description of the mechanism. Therefore, this work will continue with the detailed validation of mass transfer tests with the dissolved oxygen profiles available in the literature.

References

Buffo, A., Vanni, M., Marchisio, D.L., Comparison between different methods for the investigation of turbulent gas-liquid systems byusing multivariate population balance models, In 8th International Conference on CFD in Oil and Gas, Metallurgical and Process Industries, Trondheim, Norway (2011)

Buffo, A., Marchisio, D.L., Vanni, M., Multidimensional population balance model for the simulation of turbulent gas-liquid systems instirred tank reactors, Chemical Engineering Science, Vol. 74,31-44 (2012)

Buffo, A., Vanni, M., Marchisio, D.L., Fox, R.O., Multivariate quadrature-based moments methods for turbulent polydisperse gas-liquid systems, International Journal of Multiphase Flow, Vol. 50, 41-57(2013)

Buwa, V.V., Ranade, V.V., Dynamics of gas-liquid flow in a rectangular bubble column: experiments and single/multi-group CFD simulations, Chemical Engineering Science, Vol. 57, 4715–4736 (2002)

Clift, R., Grace, J.R., Weber, M.E., Bubbles, Drops, and Particles. Academic Press, New York (NJ), USA (1978)

Diaz, M.E., Iranzo, A., Cuadra, D., Barbero, R., Montes, F.J, Galàn, M.A., Numerical simulation of the gas-liquid flow in a laboratory scale bubble column. Influence of bubble size distribution and non-drag forces, Chemical Engineering Journal, Vol. 139, 363-379 (2008)

Geary, N.W., Rice, R.G., Bubble size prediction for rigid and flexible spargers, AIChE Journal, Vol. 37, 161–168 (1991)

Hulburt, H., Katz, S., Some problems in particle technology: A statistical mechanical formulation. Chemical Engineering Science, Vol. 19, 555–574 (1964)

Kataoka, I., Serizawa, A., Basic equations of turbulence in gas-liquid two-phase flow, International Journal of Multiphase Flow, Vol. 15, 843–855 (1989)

Laakkonen, M., Moilanen, P., Alopaeus, V., Aittamaa, J.,Modelling local bubble size distributions in agitated vessels, Chemical Engineering Science, Vol. 62, 721–740 (2007)

Lamont, J.C., Scott, D.S., An eddy cell model of mass transfer into the surfaceof a turbulent liquid, AIChE Journal, Vol. 16, 513–519 (1970)

Marchisio, D.L., Fox, R.O., Solution of population balance equations using the direct quadrature method of moments, Journal of Aerosol Science, Vol. 36, 43-73 (2005)

Marchisio, D.L., Virgil, R.D., Fox, R.O., Quadrature method of moments for aggregation-breakage processes, Journal of Colloid and Interface Science, Vol. 258, 322-334 (2003)

Montante, G., Paglianti, A., Magelli, F., Experimental analysis and computational modelling of gas-liquid stirred vessels, Chemical Engineering Research and Design, Vol. 85, 647–653 (2007)

Petitti, M., Marchisio, D.L., Vanni, M., Baldi, G., Mancini, N., Podenzani, F., Effect of drag modeling on the prediction of critical regime transitions in agitated gas-liquid reactors with bubble size distribution modeling, Multiphase Science and Technology, Vol. 21, 95-106 (2009)

Petitti, M., Nasuti, A., Marchisio, D.L., Vanni, M., Baldi, G., Mancini, M., Podenzani, F., Bubble size distribution modeling in stirred gas-liquid reactors with QMOM augmented by a new correction algorithm, AIChE Journal, Vol. 56, 36-53 (2010)

Yuan, C., Fox, R.O., Conditional quadrature method of moments for kinetic equations, Journal of Computational Physics, Vol. 230, 8216-8246(2011)